


Article

Surface Discharge Characteristics and Numerical Simulation in C_4F_7N/CO_2 Mixture

Xinfeng Yan ¹ , Xiaoli Zhou ^{1,*}, Ze Li ², Yong Qian ² and Gehao Sheng ²
¹ Department of Light Sources and Illuminating Engineering, School of Information Science and Technology, Fudan University, Shanghai 200433, China

² Department of Electrical Engineering, Shanghai Jiao Tong University, Shanghai 200240, China

* Correspondence: zhouxl@fudan.edu.cn

Abstract: The environmentally friendly gas C_4F_7N has been considered a potential replacement gas for SF_6 due to its excellent insulation. At present, research on C_4F_7N and its mixture mainly focuses on its insulation performance, but few people study its surface discharge mechanism and variation law. In order to study the surface discharge characteristics of the C_4F_7N/CO_2 mixture, a fluid model of surface discharge was established and simulated by COMSOL, which was used to study the mechanism of streamers during surface discharge, fit the expression of the maximum photon flux, analyze the influence of voltage and the dielectric constant of the insulator on discharge, and compare the surface discharge of C_4F_7N/CO_2 with that of SF_6 , providing the theoretical basis for the optical detection and reliable diagnosis of partial discharge. The results show that, under the same discharge conditions, the optical phenomenon of C_4F_7N/CO_2 discharge along the surface is more obvious than that of SF_6 , and as the applied voltage or the dielectric constant of the insulator increases, the streamer develops more quickly, the electric field becomes stronger, and the photon flux increases.

Keywords: environmentally friendly gas; surface discharge; law of change; photon flux



Citation: Yan, X.; Zhou, X.; Li, Z.; Qian, Y.; Sheng, G. Surface Discharge Characteristics and Numerical Simulation in C_4F_7N/CO_2 Mixture.

Appl. Sci. **2023**, *13*, 1409. <https://doi.org/10.3390/app13031409>

Received: 14 November 2022

Revised: 16 January 2023

Accepted: 19 January 2023

Published: 20 January 2023



Copyright: © 2023 by the authors. Licensee MDPI, Basel, Switzerland. This article is an open access article distributed under the terms and conditions of the Creative Commons Attribution (CC BY) license (<https://creativecommons.org/licenses/by/4.0/>).

1. Introduction

Partial discharge (PD) is one of the main factors affecting the stable operation of high-voltage electrical equipment, and surface discharge is a common type of PD. In high-voltage electrical equipment, when the surface of the insulator is discharged, a streamer develops along the surface of the insulator, which may eventually cause flashover on the surface of the insulator. Therefore, it is of great significance to study the mechanism and influencing factors of surface discharge. In the process of partial discharge, acoustic, optical, electrical, and thermal signals are often generated [1]. With advantages such as anti-electromagnetic interference, anti-mechanical vibration, and the high sensitivity and fast response of optical detection [2], partial-discharge-detection technology based on optical signals is an important research direction in the field of partial discharge in the future.

Currently, SF_6 is a widely used insulating gas in high-voltage electrical equipment, but SF_6 has a strong ability to absorb infrared radiation, and its global warming potential (GWP) is 23,900 times that of CO_2 [3,4], so it cannot meet the requirements of environmentally friendly power system development. Therefore, the search for an alternative to SF_6 gas has become a research hotspot in recent years. At present, alternative gases have been found, including SF_6/N_2 , SF_6/CO_2 and other sulfur hexafluoride mixture gases [5,6], as well as C_4F_7N , $C_5F_{10}O$, and other new insulation gases.

Studies have demonstrated that the insulation strength of C_4F_7N is about twice that of pure SF_6 . It is colorless, tasteless, and chemically stable at 700 °C, with liquefaction temperature at a standard atmospheric pressure of −4.7 °C and a GWP of only 2400 [7,8]. However, it also has some problems as an insulating medium, such as a high price and high toxicity. At present, these problems are mainly solved by mixing C_4F_7N with CO_2 ,

N₂, as well as other gases with lower liquefaction temperatures. In recent years, domestic and foreign scholars have carried out a lot of research on the insulation performance of C₄F₇N and gases mixed with it, which mainly focuses on the saturation vapor pressure of C₄F₇N [9], critical breakdown field strength, effective ionization coefficient [10], and the comparison of dielectric strength with SF₆ [11], but few people study the surface discharge mechanism and variation law of C₄F₇N and its mixture.

The theory of streamer discharge was first proposed by H. Raether [12], who believed that the separation of positive and negative charges in a streamer would shield the external electric field and cause a sharp enhancement of the electric field in a limited area outside the streamer head. The initial electrons needed for the streamer to move forward usually come from the photoionization of the streamer head, and whether the streamer can reach the cathode depends on the strength of the applied electric field. From the perspective of surface discharge, the authors of [13] carried out a simulation study on the surface discharge process in a SF₆/N₂ mixture and compared the influence of the dielectric constant of insulators on the surface charge density of insulators. In [14], air-gap discharge and surface discharge in the air were compared, and the processes of charge generation, electric field variation, and charge accumulation in surface discharge were studied. The surface charge characteristics of surface discharge were investigated in [15]. At present, there are limited studies on the mechanism and variation law of the discharge along the surface of C₄F₇N and the mixture with it. Table 1 shows the comparison between the existing research and this research.

Table 1. Comparison between existing research and this research.

	Existing Research	This Research
surface discharge	Concentrate on SF ₆ , SF ₆ /N ₂ , air, and other gases [15–18].	Concentrated on the mixture of C ₄ F ₇ N and CO ₂ .
C ₄ F ₇ N and its mixture	For its insulation performance and decomposition product [9,10,19,20].	For its surface discharge characteristics.

In this paper, the finite-element-simulation software COMSOL is adopted to simulate the surface discharge in the environmentally friendly gas C₄F₇N/CO₂. By resolving the drift-diffusion equation and the Poisson equation of charged particles, the mechanism and variation law of the streamer in C₄F₇N/CO₂ are obtained, and the influence of changes in voltage and the dielectric constant of the insulator on electric field intensity, electron concentration, and luminous flux was investigated. Simultaneously, the surface discharge of C₄F₇N/CO₂ is compared with that of SF₆, providing a theoretical basis for optical detection and reliable diagnosis of surface discharge in C₄F₇N/CO₂.

2. Simulation Model

To simulate the surface discharge in C₄F₇N/CO₂, physical and numerical models of surface discharge were established.

2.1. Physical Model

The physical model used in the simulation is given in Figure 1, which is mainly composed of a needle electrode, a plane electrode, and a solid insulating medium. The simulation area is the red dashed line in the figure. The needle electrode is an anode, and the plane electrode is grounded. The distance between the needle electrode and the plane electrode is 4 mm, and the size of the solid insulating medium is 4 × 4 mm.

Studies have shown that the C₄F₇N/CO₂ mixture, with C₄F₇N accounting for 7–13%, has the potential to replace SF₆ gas [21]. In this paper, a mixture of 9% C₄F₇N and 91% CO₂

is used; the temperature is 300 K, the pressure is 0.1 MPa, and the initial density distribution of electrons and positive ions is a Gaussian distribution [14]:

$$n_{e,p} = n_{\max} \times \exp\left(-\frac{(r-r_0)^2}{2s_0^2} - \frac{(z-z_0)^2}{2s_0^2}\right) \quad (1)$$

where $n_{\max} = 10^{20}$ (1/m³), (r_0, z_0) is the coordinate of the needle tip, s_0 is the radius of the initial distribution of particles ($s_0 = 25$ μm), and the initial density distribution of negative ions is set to 0. The maximum value of the initial electric field is at the junction of the needle tip, the solid dielectric, and the gas, so a large number of particles are clustered around it.

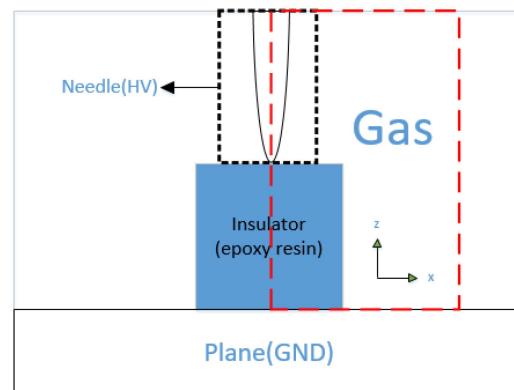


Figure 1. Structure of physical model.

2.2. Numerical Model

According to the theory of streamer discharge, streamer channels are formed during the development of streamers, and there are a large number of positive and negative ions in the streamer channels. Because the streamer channel is electrically neutral, it can be approximated as a plasma. The establishment of the fluid model [22] is based on the drift-diffusion equations of electrons, cations, and anions, which describe the generation, dissipation, and transport processes of charged particles. The specific equation [23] is as follows:

$$\frac{\partial n_e}{\partial t} + \nabla(-\mu_e n_e E - D_e \nabla n_e) = S_{ph} + \alpha n_e |\mu_e E| - \eta n_e |\mu_e E| \quad (2)$$

$$\frac{\partial n_p}{\partial t} + \nabla(-\mu_p n_p E - D_p \nabla n_p) = S_{ph} + \alpha n_e |\mu_e E| \quad (3)$$

$$\frac{\partial n_n}{\partial t} + \nabla(-\mu_n n_n E - D_n \nabla n_n) = \eta n_e n_p \quad (4)$$

where E is the electric field intensity; n_e , n_p , and n_n are the densities of electrons, cations, and anions; μ_e , μ_p and μ_n are electron, cation, and anion mobility; D_e , D_p and D_n are electron, cation, and anion diffusivity; α is the Townsend ionization coefficient; η is the Townsend adsorption coefficient; and S_{ph} is photoionization source term. The photoionization term in the drift-diffusion equation can be simplified to uniform background ionization [24,25], and the parameters involved in Equations (2)–(4) are obtained from [26].

The electric field change in the gas satisfies Poisson's equation [23], namely Equation (5). The dynamics of space charge in the insulator is completely different from that in the gas, and the transport time of the space charge in the solid is much longer than that required by the streamer [13]. Therefore, the insulator interior can be regarded as satisfying the condition of no space charge, namely Equation (6).

$$\nabla^2 V = \frac{-e(n_p - n_e - n_n)}{\epsilon_0} \quad (5)$$

$$\nabla^2 V = 0 \quad (6)$$

where e is the element charge, ε_0 is the vacuum permittivity, and V is the electric potential. Because the charge–mass ratio of electrons is much greater than that of ions, ions can be regarded as stationary for a few nanoseconds [27]. Figure 2 shows the basic flow of the surface discharge.

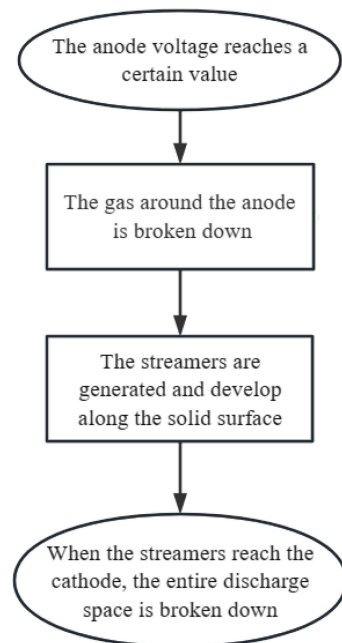


Figure 2. Flow chart of the surface discharge.

2.3. Calculation of Photon Flux

According to [28], during the discharge process, the optical radiation flux at any position is proportional to the degree of ionization at that point. This is due to the fact that the high intensity of the electric field causes the electron collision reaction between the electron and the gas molecules to be more violent, resulting in more cations, anions, excited atoms, and so on. When excited atoms or gas molecules are de-excited, they emit photons. Based on this, the calculation formula for photon flux at a point in space is as follows:

$$I = \alpha \mu_e |E| n_e \quad (7)$$

where I is the value of optical radiation flux, which ignores the lifetime of excited-state substances [23].

3. Analysis of Simulation Result

When the voltage at the needle electrode reaches a certain value, the gas around the electrode is broken down, resulting in partial discharge along the surface of the solid insulating medium. The surface discharge process of C_4F_7N/CO_2 was obtained through simulation; the effect of the applied voltage and the insulator's dielectric constant on discharge was investigated, and the surface discharge of C_4F_7N/CO_2 and SF_6 was contrasted.

3.1. Streamer Development Process

This paper analyzes the development process of streamers during surface discharge of C_4F_7N/CO_2 in three stages: Stage 1 is along the upper surface of the insulator; Stage 2 is along the rounded corner transition stage; and stage 3 is along the right surface of the insulator. Figure 3 shows the electric field intensity (V/m) of the three stages in the process of surface discharge. Figure 4 shows the potential distribution (V) at the initial stage of discharge.

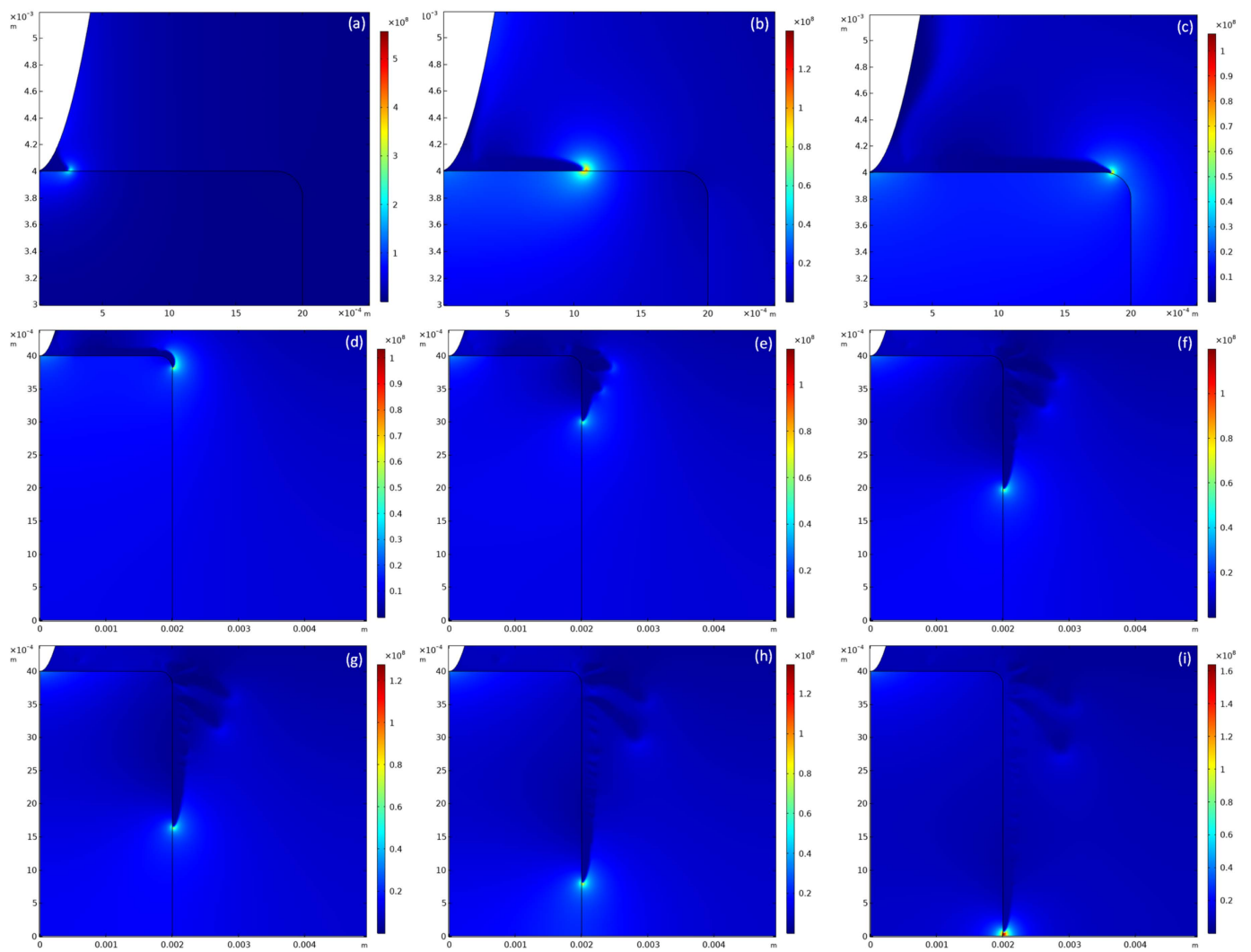


Figure 3. Surface discharge process: (a) 0.03 ns; (b) 0.2 ns; (c) 0.5 ns; (d) 0.7 ns; (e) 1.2 ns; (f) 1.7 ns; (g) 1.84 ns; (h) 2.14 ns; (i) 2.34 ns.

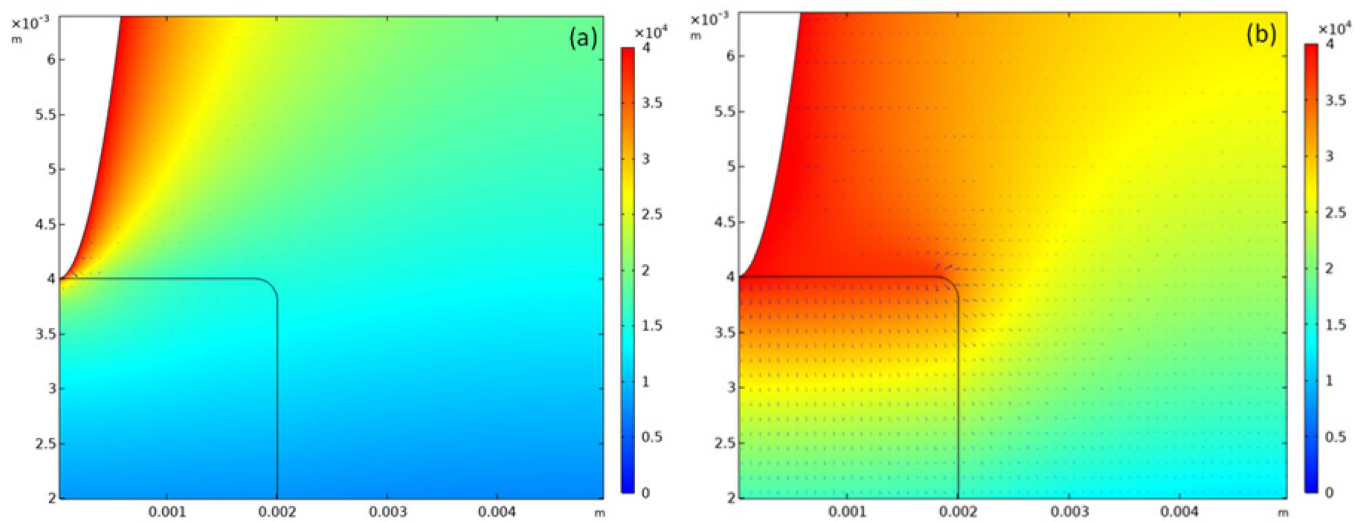


Figure 4. Potential distribution at the initial stage of discharge: (a) 0 ns; (b) 0.5 ns.

After applying voltage to the needle electrode, the electric field near the needle electrode is very strong, and a large number of electrons and cations are distributed here. The applied voltage intensifies the movement of electrons, which collides with neutral molecules in the gas mixture, such as C_4F_7N and CO_2 , and generates a large number of electrons and cations. Because the charge–mass ratio of cations is much lower than that of electrons, the movement speed of cations is much lower than that of electrons, which can be regarded as stationary within a nanosecond [27]. Under the action of the applied voltage at the needle electrode, electrons continue to move to the needle electrode, while cations almost stay in place. With the accumulation of cations, the space charge effect becomes ever more significant, and the electric field of the streamer head continues to increase. When the electric field at the head of the streamer exceeds the critical reduced field strength of the mixed gas, a new electronic collapse occurs and the streamer continues to develop, as shown in Figure 3a–c.

When the streamer is transitioning from the top surface of the insulator to the right surface along the rounded corner, the streamer-branching phenomenon occurs, as shown in Figure 3d–f, which is caused by the uneven distribution of the electric potential. By comparing (a) and (b) in Figure 4, it can be found that at 0.5 ns, the electric potential gradients along the positive x direction and the negative z direction are very large, which means the field strengths in these two directions are significantly larger than those in other directions. When the electric field intensity is higher than the critical reduced electric field intensity of the gas, the streamer develops in the direction of a large electric potential gradient. A similar streamer-branching phenomenon was observed in [27].

After the transition, the streamer continues along the right surface of the insulator, and the branched streamer gradually moves to the cathode. Because the streamer branch has a speed of x direction, this part of the streamer gradually moves away from the insulator. By comparing Figure 3g–i, in this process, the streamer branch becomes slower and eventually stops. This is because when the streamer is far away from the insulator, the electric field at the head of the streamer and the background electric field become smaller and smaller, which cannot make the streamer continue to move forward.

As the streamer is still approaching the cathode, the electric field intensity at the head of the streamer increases, while the electric field intensity at the tail of the streamer near the needle electrode also increases. This is due to the fact that a large number of electrons outside the streamer enter the streamer channel and flow to the anode, and the space charge effect weakens the electric field inside the channel to a certain extent. When the streamer reaches the cathode, the electric field intensity of the streamer head increases from 7.84×10^7 V/m to 1.07×10^8 V/m.

Figure 5 shows the variation of electric field intensity in the streamer head during discharging. In the first and second stages, when the streamer gradually moves away from the needle electrode, the field intensity gradually decreases because the development of the streamer consumes part of the energy and weakens the ionization degree of the streamer head. After the streamer transits from the upper surface to the right surface, the electric field intensity gradually increases. This is due to the fact that when the streamer develops on the right surface of the insulator, the electric potential gradient is very large and the background electric field is very strong, resulting in an intensified collision reaction of electrons and the generation of more electrons. At this time, the streamer is in a state of “accelerated motion”.

Figure 6 shows the variation of photon flux in the streamer head during discharge. During the development of the streamer, the photon flux first decreases and then increases. When the streamer reaches the cathode, the photon flux increases from 2.18×10^9 m^{−3}s^{−1} to 3.83×10^9 m^{−3}s^{−1}. By comparing Figures 4 and 5, it can be found that the variation law of photon flux is comparable to that of electric field intensity, and similar phenomena have also been observed in [29].

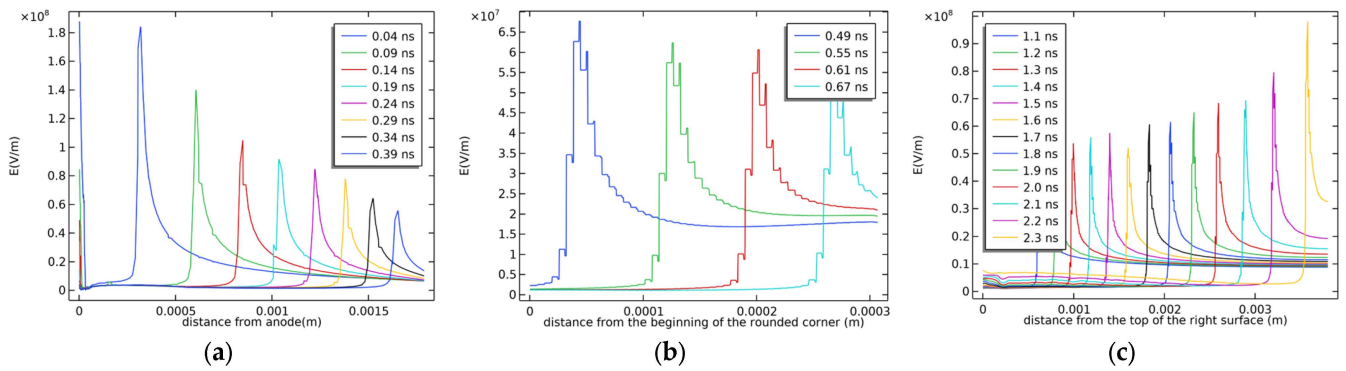


Figure 5. Variation in the electric field intensity of the streamer head. (a) Stage 1; (b) Stage 2; (c) Stage 3.

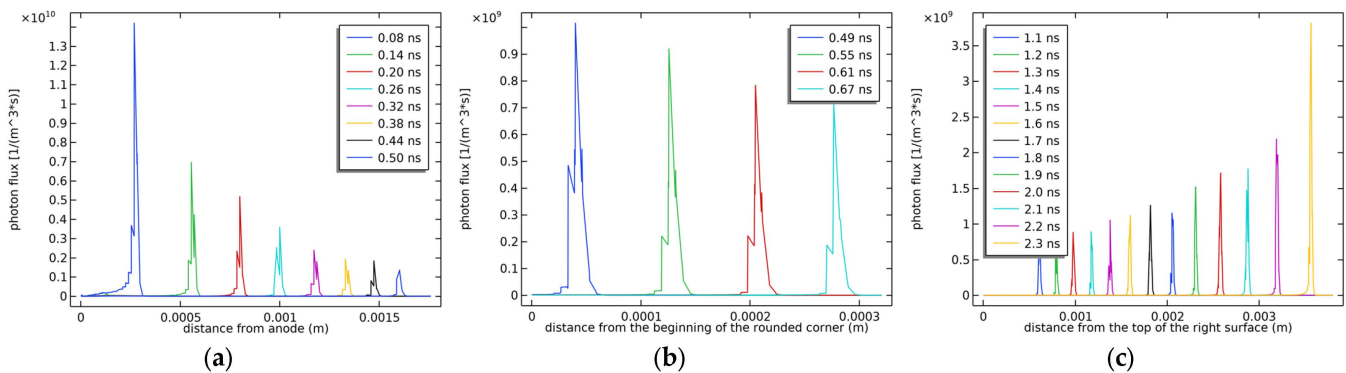


Figure 6. Variation in photon flux of the streamer head. (a) Stage 1 (b) Stage 2 (c) Stage 3.

According to the data in Figure 6a,c, the maximum photon flux can be expressed as follows:

$$I = 2.138 \times 10^{10} e^{-1899d_1} \quad (8)$$

$$I = 5.999 \times 10^8 e^{367.2d_2} + 0.6474e^{5838d_2} \quad (9)$$

where I is the photon flux, Equation (8) is the expression of stage 1, d_1 is the distance from the streamer head to the anode, Equation (9) is the expression of stage 3, and d_2 is the distance from the streamer head to the cathode.

3.2. Effect of Voltage on Discharge

In order to explore the influence of the applied voltage on the surface discharge of C_4F_7N/CO_2 , this paper compares the surface discharge of C_4F_7N/CO_2 when the applied DC voltage is 40 KV, 42.5 KV, 45 KV, and 50 KV.

Figure 7 shows the two-dimensional electron concentration distribution of the streamer near the cathode at different applied DC voltages. By comparison, as the applied DC voltage increases, the electron concentration of the streamer reaching the cathode increases from $5.53 \times 10^{21} m^{-3}$ to $1.15 \times 10^{22} m^{-3}$. At the same time, the development time of the streamer from the needle electrode to the plane electrode becomes shorter, and the gas mixture is more likely to be broken down, which is consistent with the results in [17].

Figure 8 shows the electron concentrations at the time indicated in Figure 7. Figures 9 and 10 show the electric field intensity and photon flux at the time indicated in Figure 7. With the increase in the applied voltage, the background electric field in the whole space increases, the ionization reaction of the mixed gas intensifies, and more electrons are produced. Therefore, the electric field intensity of the streamer head increases, and the photon flux also increases.

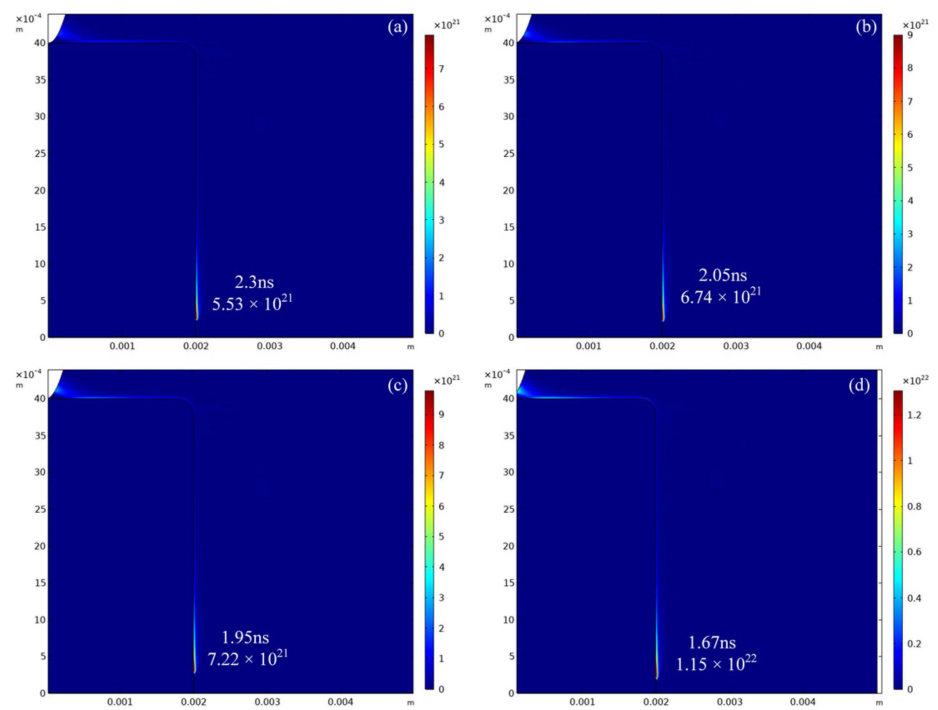


Figure 7. Electron concentrations at different applied DC voltages: (a) 40 KV; (b) 42.5 KV; (c) 45 KV; (d) 50 KV.

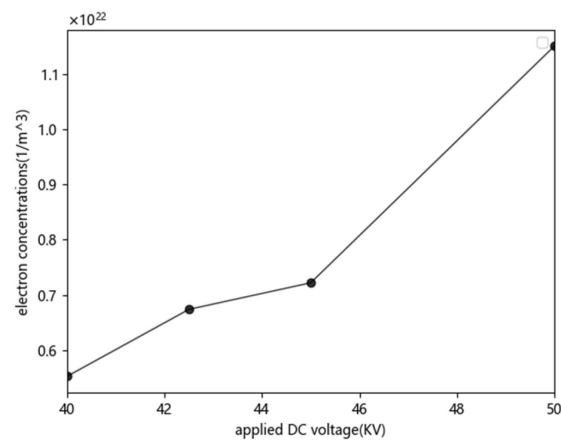


Figure 8. Variation of electron concentrations with applied DC voltage.

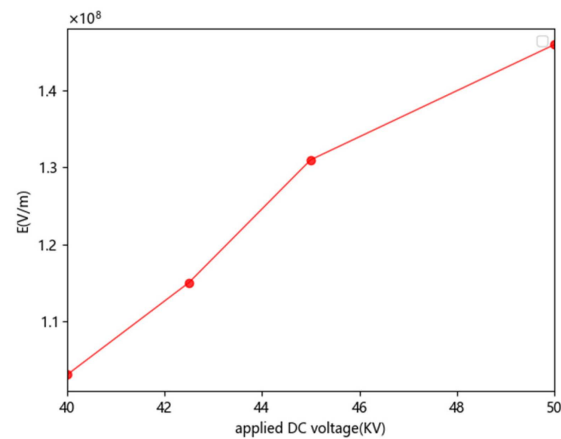


Figure 9. Variation of electric field strength with applied DC voltage.

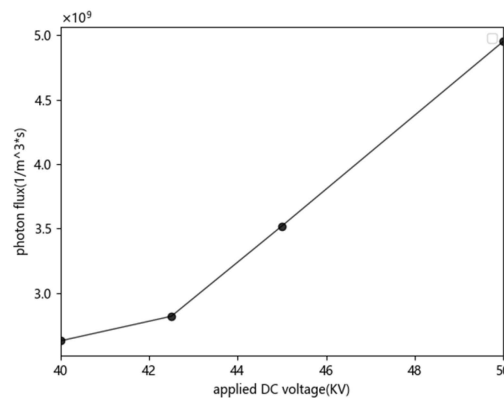


Figure 10. Variation of luminous flux with applied DC voltage.

3.3. Effect of Dielectric Constant on Discharge

In order to explore the influence of the dielectric constant of the insulator on the surface discharge of C_4F_7N/CO_2 , this paper compares the surface discharge of C_4F_7N/CO_2 when the dielectric constants are 2, 3, 4, and 5.

Figure 11 shows the two-dimensional electron concentration distribution when the streamer develops near the cathode under different dielectric constants. As the dielectric constant of the insulator increases, the electron concentration in the streamer near the cathode increases from $4.63 \times 10^{21} \text{ m}^{-3}$ to $1.16 \times 10^{22} \text{ m}^{-3}$. At the same time, the development speed of the streamer becomes faster, and the development time from the needle electrode to the plane electrode becomes shorter, which is consistent with the results in [30].

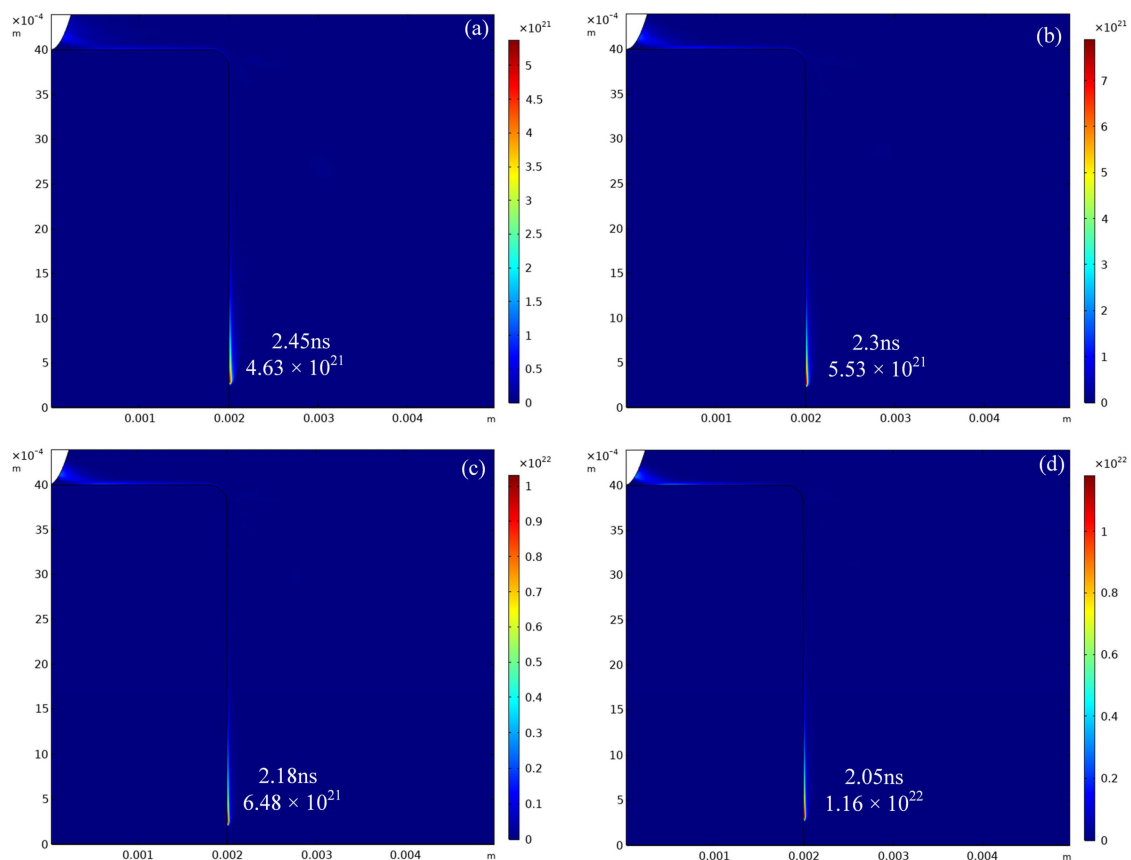


Figure 11. Electron concentrations of different dielectric constants: (a) $\epsilon_r = 2$; (b) $\epsilon_r = 3$; (c) $\epsilon_r = 4$; (d) $\epsilon_r = 5$.

Figure 12 shows the electron concentrations at the times indicated in Figure 11. Figures 13 and 14 show the electric field intensity and photon flux at the time indicated in Figure 11. The dielectric constant of the insulator becomes larger, the polarity becomes stronger, and the interaction force between the insulator and the streamer increases, resulting in a more intense ionization reaction between gas molecules. Finally, the electric field of the streamer head increases, the photon flux increases, and the development speed of the streamer becomes faster.

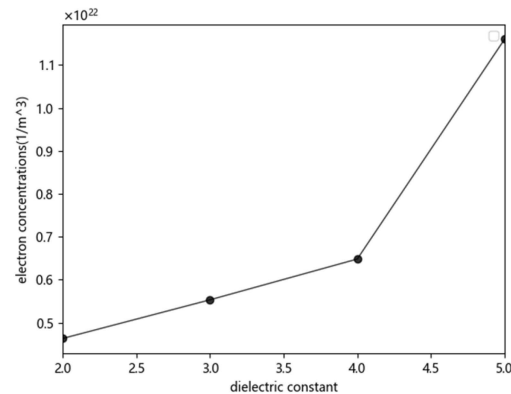


Figure 12. Variation of electron concentrations with ϵ_r .

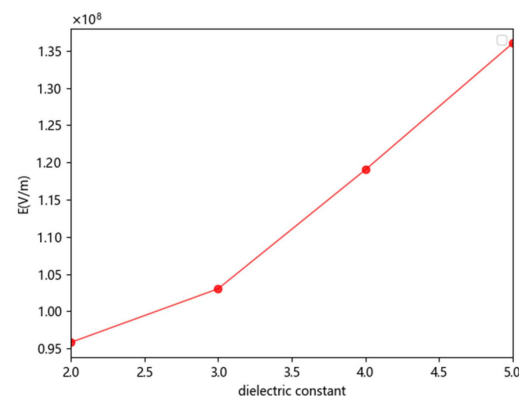


Figure 13. Variation of electric field strength with ϵ_r .

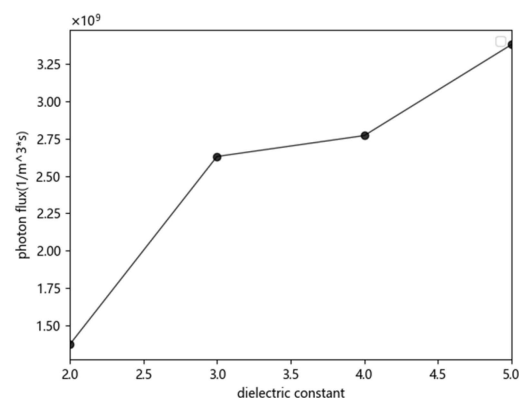


Figure 14. Variation of photon flux with ϵ_r .

3.4. Comparison with the Discharge in SF₆

More and more studies have shown that the C₄F₇N/CO₂ mixture can be an alternative to SF₆. In order to study the surface discharge laws of C₄F₇N/CO₂ and SF₆, the discharges of C₄F₇N/CO₂ and SF₆ were compared in this paper. Except for the gas medium, the other conditions were exactly alike.

Figure 15 shows the electric field intensity of three stages of surface discharge in C_4F_7N/CO_2 and SF_6 , where (a), (c), and (e) are the surface discharge in C_4F_7N/CO_2 , and (b), (d), and (f) are the surface discharge in SF_6 . By comparison, the discharge rate of C_4F_7N/CO_2 is slightly faster than that of SF_6 , and the electric field intensity of the streamer head is also greater than that of SF_6 . Figure 16 displays the electron concentrations in the three stages of surface discharge in C_4F_7N/CO_2 and SF_6 . It can be seen that in each stage of surface discharge, the electron concentration in the streamer head in C_4F_7N/CO_2 is greater than that in SF_6 .

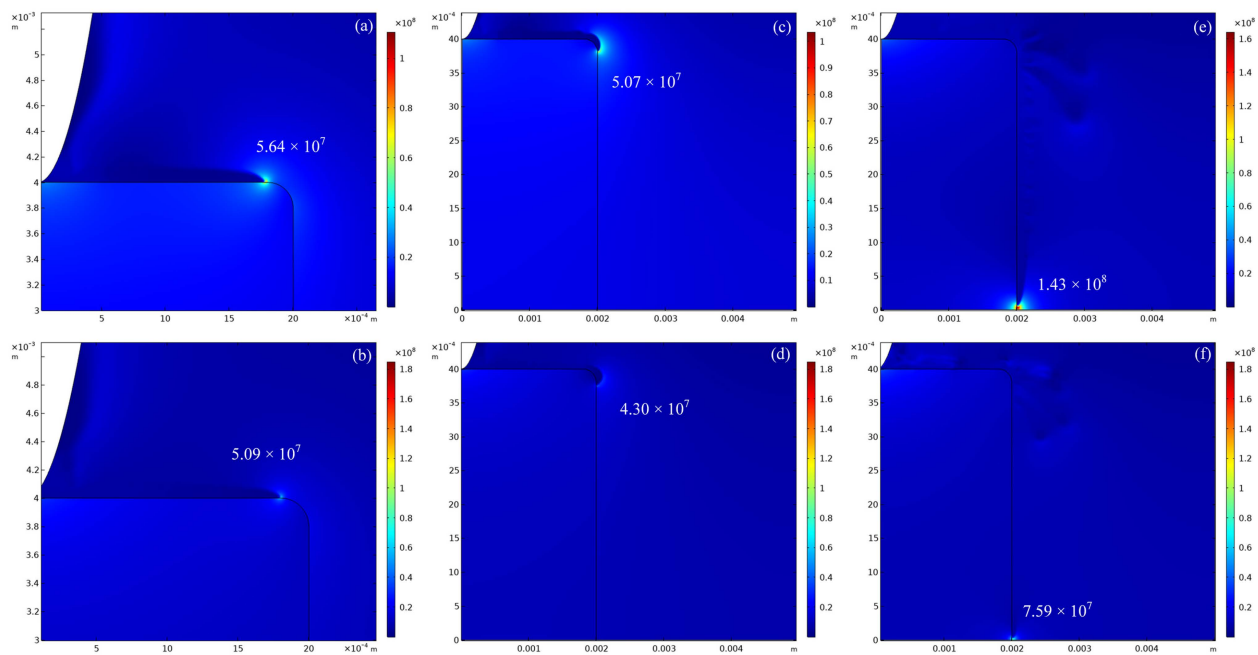


Figure 15. Comparison of the electric field intensity of surface discharge in C_4F_7N/CO_2 and SF_6 : (a) 0.45 ns; (b) 0.5 ns; (c) 0.7 ns; (d) 0.8 ns; (e) 2.34 ns; (f) 3.42 ns.

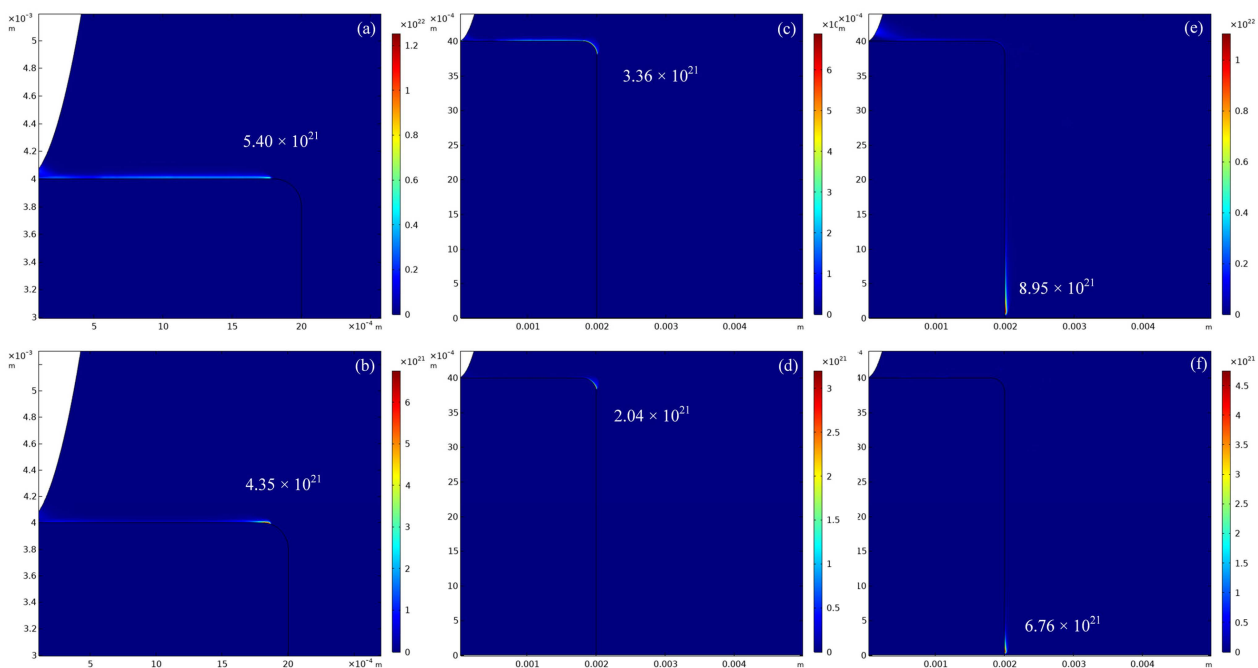


Figure 16. Comparison of electron concentrations for surface discharge in C_4F_7N/CO_2 and SF_6 : (a) 0.45 ns; (b) 0.5 ns; (c) 0.7 ns; (d) 0.8 ns; (e) 2.34 ns; (f) 3.42 ns.

Table 2 summarizes the data in Figures 15 and 16. It can also be seen from Figures 15 and 16 and Table 2 that the streamer channel in C_4F_7N/CO_2 is more obvious than that in SF_6 . The streamer channel is formed because electrons are constantly moving towards the anode. The electric field generated by the electrons and cations is opposite to that of the needle electrode, so the electric field inside the streamer channel is small. Because the electron concentration in C_4F_7N/CO_2 is greater than that in SF_6 , the streamer channel in C_4F_7N/CO_2 is more noticeable than that in SF_6 .

Table 2. The data in Figures 12 and 13.

	Stage 1	Stage 2	Stage 3
C_4F_7N/CO_2	5.64×10^7 V/m	5.07×10^7 V/m	1.43×10^8 V/m
SF_6	5.09×10^7 V/m	4.30×10^7 V/m	7.59×10^7 V/m
C_4F_7N/CO_2	5.40×10^{21} m ⁻³	3.36×10^{21} m ⁻³	8.95×10^{21} m ⁻³
SF_6	4.35×10^{21} m ⁻³	2.04×10^{21} m ⁻³	6.76×10^{21} m ⁻³

Figure 17 shows the photon flux of surface discharge in SF_6 . When comparing Figures 6 and 17, it is clear that the photon flux in C_4F_7N/CO_2 is greater than that in SF_6 , regardless of stage 1, stage 2, or stage 3. This demonstrates that optical methods can be used to detect surface discharge in C_4F_7N/CO_2 when it replaces SF_6 as the insulating gas for high-voltage electrical equipment in the future.

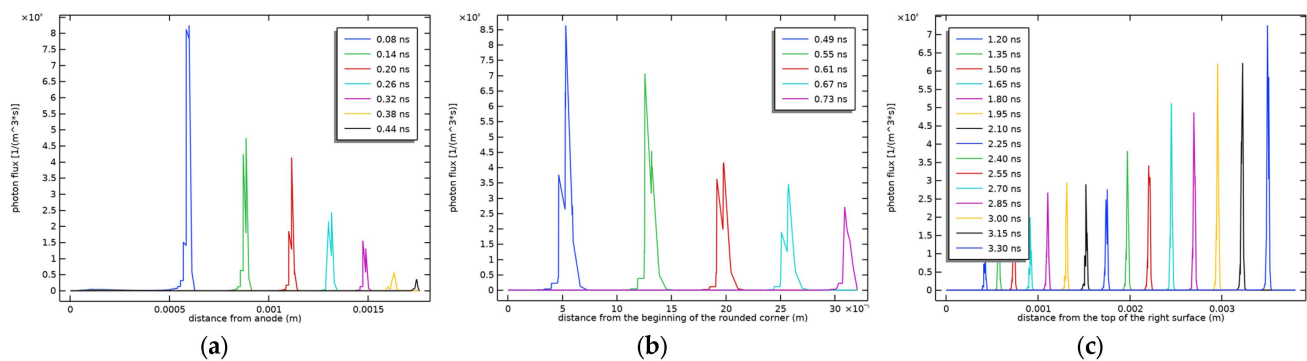


Figure 17. Variation in photon flux of the streamer head in SF_6 . (a) Stage 1; (b); Stage 2 (c); Stage 3.

4. Conclusions

In this paper, the surface discharge process in a C_4F_7N/CO_2 gas mixture is obtained by COMSOL simulation. On this basis, the influence of the applied voltage and dielectric constant of the insulator on the discharge is studied, and the surface discharges in C_4F_7N/CO_2 and SF_6 are compared, which provides a theoretical basis for the optical detection of surface discharge in the environmentally friendly gas C_4F_7N/CO_2 . The following are the main conclusions:

1. Surface discharge in C_4F_7N/CO_2 can be divided into three stages: it develops along the upper surface of the insulator, transitions along the rounded corner, and develops along the right surface of the insulator. The streamer branch appears during the transition phase, develops for a short time, and then stops in the third phase.
2. When the streamer reaches the vicinity of the cathode, the electric field intensity increases from 7.84×10^7 V/m to 1.07×10^8 V/m, the photon flux increases from 2.18×10^9 m⁻³s⁻¹ to 3.83×10^9 m⁻³s⁻¹, and the change law of the photon flux is similar to that of the electric field intensity. The expression of the maximum photon flux by fitting is $I = 2.138 \times 10^{10} e^{-1899d_1}$ (stage 1) and $I = 5.999 \times 10^8 e^{367.2d_2} + 0.6474e^{5838d_2}$ (stage 3).
3. As the applied voltage increases, the peak of electric field intensity and the peak of photon flux in the streamer head increase, and the streamer growth speed increases.

4. The peak electric field intensity of the streamer head likewise increases along with the insulator's increased dielectric constant, which further accelerates the streamer's development.
5. As an alternative to SF₆, C₄F₇N/CO₂ has a similar surface discharge phenomenon and a slightly faster discharge rate than that of SF₆. The electric field intensity, electron concentration, and photon flux generated by discharge in C₄F₇N/CO₂ are higher than those in SF₆, and the streamer channel is also more obvious than that in SF₆.

Author Contributions: Conceptualization, X.Y.; methodology, X.Y.; software, X.Y.; formal analysis, X.Y.; data curation, X.Y.; supervision, X.Z., Z.L., Y.Q. and G.S. All authors have read and agreed to the published version of the manuscript.

Funding: This research was funded by the National Natural Science Foundation of China (NO. 62075045).

Data Availability Statement: Data sharing not applicable.

Conflicts of Interest: The authors declare no conflict of interest.

References

1. Stone, G.C. Partial discharge diagnostics and electrical equipment insulation condition assessment. *IEEE Trans. Dielectr. Electr. Insul.* **2005**, *12*, 891–904. [\[CrossRef\]](#)
2. Zang, Y.; Qian, Y.; Wang, H.; Xu, A.; Sheng, G.; Jiang, X. Method of GIL partial discharge localization based on natural neighbor interpolation and ECOC-MLP-SVM using optical simulation technology. *High Volt.* **2021**, *6*, 514–524. [\[CrossRef\]](#)
3. Yu, Z.; Wenjun, Z.; Jianhui, Y.; Shizhuo, H.; Tianran, Z. Analysis on application characteristics of environmental insulated mixed gases. *Guangdong Electr. Power* **2018**, *31*, 3–8.
4. Hu, S.; Wenjun, Z.; Jianhui, Y. Application of quantitative structure-property relationship model in research on SF₆ alternative gases. *Guangdong Electr. Power* **2018**, *31*, 9–17.
5. Qin, Z.; Zheng, Y.; Wei, L.; Yang, S.; Zhang, C.; Zhou, W. Impulse insulation property of SF₆/N₂ mixture under low temperatures. *High Volt. Eng.* **2017**, *43*, 3907–3913.
6. Zhao, S.; Jiao, J.; Zhao, X.; Zhang, H.; Xiao, D.; Yan, J.D. Synergistic effect of SF₆/N₂ gas mixtures in slightly non-uniform electric field under lightning impulse. *High Volt. Eng.* **2016**, *42*, 635–641.
7. Zhang, X.; Tian, S.; Xiao, S.; Deng, Z.; Li, Y.; Tang, J. Insulation strength and decomposition characteristics of a C₆F₁₂O and N₂ gas mixture. *Energies* **2017**, *10*, 1170. [\[CrossRef\]](#)
8. Okabe, S.; Ueta, G.; Utsumi, T.; Nukaga, J. Insulation characteristics of GIS insulators under lightning impulse with DC voltage superimposed. *IEEE Trans. Dielectr. Electr. Insul.* **2015**, *22*, 3269–3277. [\[CrossRef\]](#)
9. Li, X.; Deng, Y.; Jiang, X.; Zhao, H.; Zhuo, R.; Wang, D.B.; Fu, M.L. Insulation performance and application of environment-friendly gases mixtures of C₄F₇N and C₅F₁₀O with CO₂. *High Volt. Eng.* **2017**, *43*, 708–714.
10. Nechmi, H.E.; Beroual, A.; Girodet, A.; Vinson, P. Effective ionization coefficients and limiting field strength of fluoronitriles-CO₂ mixtures. *IEEE Trans. Dielectr. Electr. Insul.* **2017**, *24*, 886–892. [\[CrossRef\]](#)
11. Kieffel, Y.; Irwin, T.; Ponchon, P.; Owens, J. Green gas to replace SF₆ in electrical grids. *IEEE Power Energy Mag.* **2016**, *14*, 32–39. [\[CrossRef\]](#)
12. Raether, H. Die entwicklung der elektronenlawine in den funkenkanal. *Z. Phys.* **1939**, *112*, 464–489. [\[CrossRef\]](#)
13. Sima, W.X.; Shi, J.; Yang, Q. Surface discharge simulation in SF₆ and N₂ mixtures with a plasma chemical model. *Surf. Rev. Lett.* **2014**, *21*, 1450010. [\[CrossRef\]](#)
14. Tran, T.N.; Golosnoy, I.O.; Lewin, P.L.; Georgiou, G.E. Numerical modelling of negative discharges in air with experimental validation. *J. Phys. D Appl. Phys.* **2010**, *44*, 015203. [\[CrossRef\]](#)
15. Li, X.; Sun, A.; Teunissen, J. A computational study of negative surface discharges: Characteristics of surface streamers and surface charges. *IEEE Trans. Dielectr. Electr. Insul.* **2020**, *27*, 1178–1186. [\[CrossRef\]](#)
16. Zhiqiang, H.; Ruochen, G.; Junhao, L. Surface partial discharge characteristics of SF₆/N₂ Gas mixture at DC Voltage. *Trans. China Electrotech. Soc.* **2020**, *35*, 3087–3096.
17. Zhiqiang, H.; Shanyuan, S.; Ruochen, G.U.O.; Peichuan, P.; Junhao, L.I. Surface partial discharge characteristics of SF₆ gas at DC Voltage. *High Volt. Technol.* **2020**, *46*, 1643–1651.
18. Jee, S.; Lim, D. Surface discharge mechanism with a change of gas pressure in N₂/O₂ mixed gas for insulation design of SF₆-free high-voltage power equipment. *IEEE Trans. Dielectr. Electr. Insul.* **2021**, *28*, 771–779. [\[CrossRef\]](#)
19. Liu, W.; Zhao, Y.; Zhang, Y.; Yan, J.; Zhu, Z.H. Study on theoretical analysis of C₄F₇N infrared spectra and detection method of mixing ratio of the gas mixture. *J. Mol. Spectrosc.* **2021**, *381*, 111521. [\[CrossRef\]](#)
20. Zhang, X.; Zhang, Y.; Huang, Y.; Li, Y.; Cheng, H.; Xiao, S. Detection of decomposition products of C₄F₇N-CO₂ gas mixture based on infrared spectroscopy. *Vib. Spectrosc.* **2020**, *110*, 103114. [\[CrossRef\]](#)
21. Lingzhi, W.; Wenjun, Z.; Tianshi, Z.; Wei, L.; Shizhuo, H.; Jianhui, Y. Power frequency insulation properties of C₄F₇N/CO₂ mixture gas under homogeneous and extremely heterogeneous electric fields. *High Volt. Technol.* **2019**, *45*, 1101–1107.

22. Naidis, G.V. Positive and negative streamers in air: Velocity-diameter relation. *Phys. Rev. E* **2009**, *79*, 057401. [[CrossRef](#)] [[PubMed](#)]
23. Yiming, Z.; Yong, Q.; Wei, L. Simulation study on streamer of tip defects in C₄F₇N/CO₂ mixed gas. *Trans. China Electrotech. Soc.* **2020**, *35*, 34–42.
24. Luo, B.; He, H.; Cheng, C.; Xia, S.; Du, W.; Bian, K.; Chen, W. Numerical simulation of the positive streamer propagation and chemical reactions in SF₆/N₂ mixtures under non-uniform field. *IEEE Trans. Dielectr. Electr. Insul.* **2020**, *27*, 782–790. [[CrossRef](#)]
25. Dhali, S.K.; Pal, A.K. Numerical simulation of streamers in SF₆. *J. Appl. Phys.* **1988**, *63*, 1355–1362. [[CrossRef](#)]
26. Zhang, J.; Sinha, N.; Jiang, M.; Wang, H.; Li, Y.; Antony, B.; Liu, C. DC breakdown characteristics of C₄F₇N/CO₂ mixtures with particle-in-cell simulation. *IEEE Trans. Dielectr. Electr. Insul.* **2022**, *29*, 1005–1010. [[CrossRef](#)]
27. Hua, W.; Fukagata, K. Near-surface electron transport and its influence on the discharge structure of nanosecond-pulsed dielectric-barrier-discharge under different electrode polarities. *Phys. Plasmas* **2019**, *26*, 013514. [[CrossRef](#)]
28. Morrow, R.; Lowke, J.J. Streamer propagation in air. *J. Phys. D Appl. Phys.* **1999**, *30*, 614. [[CrossRef](#)]
29. Zhao, L.; Zang, Y.; Liu, W.; Qian, Y.; Zhou, X. Two-dimensional simulation of transition from primary to secondary streamer discharge in air. *AIP Adv.* **2019**, *9*, 095028. [[CrossRef](#)]
30. Sobota, A.; Lebouvier, A.; Kramer, N.J.; Van Veldhuizen, E.M.; Stoffels, W.W.; Manders, F.; Haverlag, M. Speed of streamers in argon over a flat surface of a dielectric. *J. Phys. D Appl. Phys.* **2009**, *42*, 015211. [[CrossRef](#)]

Disclaimer/Publisher’s Note: The statements, opinions and data contained in all publications are solely those of the individual author(s) and contributor(s) and not of MDPI and/or the editor(s). MDPI and/or the editor(s) disclaim responsibility for any injury to people or property resulting from any ideas, methods, instructions or products referred to in the content.